JPTQ Decoction Inhibits Tumor Proliferation and Lung Metastasis in Tumor-bearing Mice with Triple Negative Breast Cancer

Jin Zhang (bihaiyinsha0419@163.com)
Zhejiang Chinese Medical University
Biyu Cai
Zhejiang Chinese Medical University
Chenxiao Ye
Zhejiang Chinese Medical University
Xinrong Li
Zhejiang Chinese Medical University
Haitao Chen
Cancer Hospital of university of chinese academy of sciences/Zhejiang Cancer Hospital
Yi Lu
Cancer Hospital of university of Chinese Academy of Sciences/Zhejiang Cancer Hospital
Zhili Xu
Zhejiang Chinese Medical University
Qinghua Yao
Cancer Hospital of university of Chinese Academy of Sciences/Zhejiang Cancer hospital
Yong Guo
The First Affiliated Hospital of Zhejiang Chinese medical university

Research Article

Keywords: Triple negative breast cancer, Traditionnalchinesemedcine, metastasis, EMT, Immune microenvironments.

Posted Date: December 29th, 2021

DOI: https://doi.org/10.21203/rs.3.rs-1203788/v1

Abstract

Background.

With the increasing incidence of breast cancer and the integration of multiple methods in the treatment, traditional Chinese medicine plays an increasingly important role in the comprehensive treatment of breast cancer. we aimed to determine the anti-cancer metastasis effect of Jianpi Tiaoqi Decoction (JPTQ) on breast cancer-bearing mice by monitoring the effects of its on tumor proliferation, apoptosis, angiogenesis, epithelial to mesenchymal transition (EMT) process and regulation of immune microenvironment.

Methods.

The general phenotype of the Cancer-bearing mice was monitored. Bioluminescence-imaging was performed to assess the tumor status and the metastatic status of other organs. We investigated its mechanism of the effect through transcriptome analysis, Flow Cytometry(FCM) was used to analyze peripheralblood $CD4^+$ T cells, spleen T helper 1 (Th1) cell, the proportion of MDSCs in lung. The changes of EMT process, vascular endothelial growth factor (VEGF) and Ki-67, Caspase-3 and Bcl-2 were detected by quantitative real time polymerase chain reaction (q-PCR), western blot (WB) or immunohistochemistry (IHC).

Results.

JPTQ inhibited the tumors proliferation and reduced lung metastasis. The transcriptome analysis of lung and tumor tissues indicated that EMT-related genes, angiogenesis, proliferation and apoptosis genes were regulated in JPTQ group, and the Kyoto Encyclopedia of Genes and Genomes (KEGG) analysis observed enrichment of immune-related pathways. FCM suggested that JPTQ could reduced the proportion of M-MDSCs in the lung, and increased peripheral blood $CD4^+$ T cells and Th1 cells in spleen. The q-PCR, WB or IHC assay demonstrated that E-cadherin was up-regulated in lung and tumor tissue, and Snail was down-regulated, the expression of matrix metalloprotein-9(MMP-9)was down-regulated in lung tissue. IHC showed the down-regulation of Ki67 and VEGF in lung and tumo tissues. WB found that Cleved-Caspase3 was significantly up-regulated, while Bcl-2 was down-regulated.

Conclution.

JPTQ can inhibit proliferation, angiogenesis, promote apoptosis and improve the immune microenvironment, and reverse the EMT process to inhibit the proliferation and metastasis of TNBC.

1. Introduction

Breast cancer (BC) is the most common female tumor disease, and its morbidity and mortality rate are increasing year by year, resulting in an increasing social and economic burden. In 2020, BC has overtaken lung cancer as the most frequently diagnosed cancer in women,, according to the latest global cancer burden data for 2020 released by the World Health Organization's International Agency for Research on Cancer (IARC) [1].

The triple negative breast cancer (TNBC) is an aggressive type of BC with limited treatment options [2, 3], therefore, its clinical prognosis is poor, and most patients face the risk of treatment failure. In addition, the main causes of common BC treatment failure and poor prognosis also include higher tumor load or tumor invasion and metastasis [4].

Tumor proliferation and metastasis is a complex multistep process that includes degradation of extracellular matrix (ECM), tumor angiogenesis, cell migration, invasion, cell adhesion, and reduced regulation of apoptosis [5]. In addition, EMT also plays a crucial role in the proliferation and metastasis of BC, leading to poor prognosis and drug resistance [6, 7]. EMT is characterized by deletion of EMT-associated protein E-cadherin and upregulation of interstitial associated protein N-cadherin and Vimentin [8]. The massive production of EMT and MMPs is the key cause of tumor invasion and metastasis [6]. MMP-9 is highly expressed in malignant tumors, and has a profound impact on cancer progression by affecting angiogenesis, invasion, and migration [9]. Stabilization and degradation of Snail family proteins are crucial to the regulation of EMT-related gene expression [10], high Snail expression is associated with poorer prognosis in BC [11]. Ki-67 is considered to be a typical proliferation marker, it is essential for prognostic grading and clinical decision-making [12, 13]. Angiogenesis is an important marker of cancer associated with metastasis and poor prognosis [14], inhibition of tumor growth by interfering with the binding of VEGF and VEGF receptor has become a promising therapeutic strategy [15]. In a study of 122 BC patients, caspase-3 expression was positively correlated with prognosis and metastatic status, while Bcl-2 expression was negatively correlated [16]. These findings suggest that inhibition of angiogenesis, inhibition of EMT activation and induction of apoptosis may be an effective way to treat cancer.

In recent years, the application of Tumor Immune Microenvironment (TIME) in Tumor therapy has attracted more and more attention. In TIME, T cells mainly play the adaptive immune function through effector T helper cells. Effector T helper cells include Th1,Th2, and Th17 cells, all belonging to the $CD4^+$ T cell lineage. Some CD4 subsets, notably Th2 and regulatory T cells (Treg), are known to negatively affect the anti-tumor response by reducing antigen presentation and inhibiting T cell effector function respectively [17, 18]. Interferon γ (IFNγ) secreted by activated Th1 cells acted directly on tumor cells and induced apoptosis, senescence and proliferation arrest. T helper 2 cell (Th2) secrete Interleukin 4 (IL-4), which leads to the phosphorylation of immunosuppressive signal transducer and activator of transcription 6 (STAT6), thereby promoting tumor growth and metastasis [19, 20]. The balance between IFN-γ and IL-4 feedback loops is critical for the balance between Th1 and Th2 $CD4^+$ T cell immune responses. Myeloid derived suppressor cells (MDSCs) are considered to be a group of heterogenous immune cells from the myeloid system that proliferate in pathological states such as cancer and chronic infectious diseases [21]. MDSCs are divided into two groups, $CD14^+$ monocytes (M-MDSCs) or $CD15^+$

granulocytes and polymorphic cells (PMN-MDSCs) [22]. Both M-MDSCs and PMN-MDSCs showed strong negative associations with patient survival [23]. These cells exert immunosuppressive effects to change TIME through some inhibitory products, such as argininase, Indole-2,3 dioxygenase (IDO) and inducible nitric oxide synthase (iNOS), and indirectly induce regulatory T cells(Treg)to inhibit the immune response of the body, leading to tumor growth and development [21, 24]. Therefore, understanding the cellular heterogeneity of immunoinfiltrating cells and its mechanism is of great importance for optimizing existing therapeutic methods and discovering new therapeutic targets.

Some traditional treatment methods of BC have made progress in the past decades, but its side effects and drug resistance lead to poor quality of life and poor survival outcomes [25]. Some emerging therapies, such as molecular targeted therapy and immunotherapy, benefit only specific groups of BC patients, and these conditions have become the bottleneck in the treatment of BC [26, 27]. Therefore, it is urgent to develop some new drugs with high efficiency, low toxicity and multiple targets for BC.

Traditional Chinese medicine (TCM) has been used in China for thousands of years. TCM treatment of BC has many advantages, such as a wide range of sources, low cost, less side effects, and multiple targets. Compared with radiotherapy and chemotherapy, it has advantages in preventing tumor recurrence and metastasis [28, 29]. Therefore, the development and application of TCM has become a hot spot in cancer research. The JPTQ decoction evaluated in this study consists of 7 kinds of Chinese herbal medicine (Table 1). At present, it has been widely used to relieve the discomfort reaction caused by radiotherapy and chemotherapy of BC, as well as other related diseases such as decreased appetite, weakness, anemia, and can regulate the immune state of BC patients. Although JPTQ has not traditionally been used for the treatment of BC, some of its active components, such as resveratrol [30], genistein [31], galangin [32], and quinic acid [33], have been shown to have anti-tumor and anti-metastatic effects in different tumor models.

In this study, we have verified the anti-TNBC proliferation and metastasis effect of JPTQ by experimental methods, and its effect is related to anti-angiogenesis, anti-proliferation, promoting cell apoptosis, reversing the EMT process, and improving the negative immune microenvironment. The conclusion of this experiment has deepened our understanding of the mechanism of this formula in the treatment of TNBC.

2. Materials And Methods

2.1 Preparation of the Extracts for JPTQ

JPTQ decoction is made up of 7 herbs, including Codonopsis pilosula, Poria cocos, Rhizoma Atractylodis Macrocephalae, Radix Glycyrrhizae, Akebiae Fructus, Radix Curcumae, lophatherum gracile (Table 1). The 7 chinese herbal medicine were soaked in 10 times distilled water for 0.5h, then decocted in distilled water in two times, combined with the decocting liquid twice, filtered and concentrated to the crude drug content of 1.6g/ml, and stored in 4℃. All the herbs were purchased from the Clinic Department of

Zhejiang Chinese Medical University (Hangzhou, China) and identified by the Department of Pharmacy, Clinic Department of Zhejiang Chinese Medical University.

Table 1 Main composition of JPTQ decoction

Main composition	Latin scientifc name	Appearance	Parts used	Amount (g)
Dangshen	Codonopsispilosula		root	15g
Fulin	Poriacocos		rhizome	15g
Baizhu	RhizomaAtractylodisMacrocephalae		rhizome	12g
Gancao	Radix Glycyrrhizae		rhizome	6g
Yuzhizi	Akebiae Fructus		fruit	15g
Yujin	Radix Curcumae		root	12g
Danzhuye	lophatherum gracile		leaf	6g

2.2 High Performance Liquid Chromatography and Mass Spectrometry (HPLC-MS) Analysis of JPTQ Decoction

To analyze the composition of the drug in the prescription, identification of Chemical Constituents in JPTQ decoction based on Q-Orbitrap High Resolution Liquid/Mass spectrometry analysis were performed.

The data of HPLC-MS analysis were preliminarily sorted out by software CD2.1 (Thermo Fisher, USA), and then retrieved and compared with the compounds database (mzcloud, mzvault, chemspider) to clarify the information of drug components in the prescription.

2.3 Breast Cancer Cellline and Culture Conditions

Mice mammary cancer cells 4T1 cellline were obtained from the Cell Bank of the Chinese Academy of Sciences (Shanghai, China) and incubated in RPMI 1640 medium (Gibco, New York, USA) containing 10% fetal bovine serum (Gibco, New York, USA) and 1% penicillin/streptomycin (Invitrogen, New York, USA) in a humidified incubator at 37◦C and 5% CO_2.

2.4 Animal Care and Experimental Protocols

Female BALB/c mice (6–8 weeks old, 18–20g) were obtained from Shanghai Sippr-BK Laboratory Animal Co. Ltd. Mice were kept in the experimental animal research center of Zhejiang Chinese medical University, at standard temperature (25 ± 2◦C) with relative humidity of 60 ± 15%, and 12h light-dark cycle. Animals were given food and water freely. After acclimation for 1 week, 4T1 cells (1 x 10^5 cells) were injected into penultimate breast fat pad on the right side of the mice. When tumors size reached a volume of 50 mm^3, the mice were divided randomly into Model group and JPTQ group and intervention began, with 8 mice in each group. According to the equivalent dose of human and mouse [34], the mice in JPTQ group were given JPTQ decoction by gavage 0.3ml/d, with the concentration of 1.6g/ml, once a day for 28 days,while the mice in control group were given the same amount of saline. Body weight and tumor volume were recorded every 3 days. The body weight of mice was measured by the average of three measurements, tumor volumes were measured with a slide caliper and calculated by the following formula:

$$Tumorvolume = (a*b^2)/2 \quad (1)$$

where a is the larger and b is the smaller of the 2 dimensions [35]. On the 29th day, after sacrifice, tumor tissue, lung tissue, peripheral blood and spleen were obtained for follow-up experiments. No adverse events were observed. All animal experiments were approved by the experimental animal ethics committee of Zhejiang Chinese Medical University.

2.5 Animal Fluorescence Imaging in vivo

For monitor the growth status of subcutaneous implant tumors and the metastases of body cavity organs, on the 0 day, the 14th day and the 28th day after tumor forming (one week later of implantion), the tumor growth was observed by in vivo bioluminescent imaging (In Vivo Imaging System-IVIS, Xenogen, CT, USA). 15 min before imaging, the mice were injected with D-luciferin (15 mg/ml in DPBS, PerkinElmer, MA, USA). Animals were received continuous exposure to 2.5% isoflurane to sustain sedation during imaging. Regions of interest from displayed images were identified and were quantified as total photon counts or photons/s using Living Image® software 4.0 (Caliper, Alameda, CA,USA).

2.6 RNA Sequencing

Total RNA was extracted using the Illumina Gene Expression Sample Prep Kit (Illumina, Inc., San Diego,CA,USA) according to the manufacturer's protocol. Quality and quantity analyses of total RNA, DGE library preparation, and sequencing were carried out at LianChuan Genomics Co., Ltd. (Hangzhou, China; Project ID: 2021B02jywA00-A34). We used a false discovery rate (FDR)≤0.05 and the absolute value of log2 ratio≥1 as the thresholds to judge the signifcance of gene expression diferences.

2.7 Detection of Tumor Immune Microenvironment by Flow Cytometry

Preparation of the sample: Mouse spleens were grinded to obtain single-cell suspension, and then 2ml cell suspension was slowly added to 3ml Ficoll-Hypaque Media, centrifuged at 400g at 18℃ for 30 min.

Monocytes were transferred to a sterile centrifuge tube and washed in PBS solution, centrifuged at 500g for 15 min, removed supernatant, the cells were resuspended in the appropriate medium.

FCM analysis of peripheralblood T lymphocytes using the following antibodies: Anti-Mouse CD4, FITC(Lot No.AM00401), Anti-Mouse CD3, PerCP-Cy5.5(Lot No.AM003E07), the two antibodies were purchased from MultiSciences Biotech (Hangzhou, China). The cells were incubated for 30 min at 22 ℃. Single cells were firstly gated for $CD3^+$ cell, then the $CD4^+$ cell were selected.

MDSCs in single cell suspension of lung tissue were analyzed with the following antibodies: Anti-Mouse CD45, APC (Lot No.AM04505), 7-AAD (Lot No.AP104-30), Anti Mouse CD11b, FITC (Lot No.AH011B01), Anti-Mouse Ly-6G /Gr-1-PE(Lot No.AM0L604), the antibodies mentioned above were purchased from MultiSciences Biotech (Hangzhou, China). Anti-Mouse Ly-6C-eFluor 780 antibody was purchased from eBioscience™ (Lot No. 47-5932-82, Massachusetts, USA), gated setting: PMN-MDSC□Single cell, live, CD45+Ly6CintLy6G+CD11b+; M-MDSC: Single cell, live, CD45+Ly6ChiLy6G-CD11b+.

Mouse Th1/Th2 Staining Kit (Lot No.KTH201, MultiSciences Biotech) was used to classify Th1/2 cells in single cell suspension of spleen. The operation process was in accordance with the protocol provided by the reagent manufacturer. gated setting: Single cell, CD3-FITC; CD4-PerCP- Cy5.5; INF-γ-PE, IL-4-APC.

The cell samples were analyzed by FCM (attune NxT,Thermo Fisher Scientific, Waltham,USA), at least 20,000 events were scored and analyzed with Attune NxT Software version 3.2.1.

2.8 Histopathological Assessment and Immunohistochemistry Assay

The Lung tissue with metastasis and tumor tissue samples were fixed in 4% paraformaldehyde then embedded in paraffin, and sectioned in 4-μm-thick slices, these sections were deparaffinized andthen stained with hematoxylin and eosin (HE). The morphological alteration was observed under microscope. For IHC analysis, the tumor sections and lung sections (4μm thick) were blocked and incubated with anti-E-cadherin (1:300,ab1416), anti-vimentin(1:500, ab8978), anti-Ki-67(1:500,ab15580), anti-VEGF (1:250, ab32152) antibodies overnight in 4℃, all four antibodies were purchased from abcam company (Cambridge,UK). Subsequently, immunostaining was performed according to the standard protocol using a DAB Substrate Kit. The sections were counterstained with hematoxylin and analyzed under an Olympus microscope (Tokyo, Japan). The quantitative analysis of IHC was measured in 5 random fields per tumor by light microscopy at a magnification of 200 and quantitated by Image-Pro Plus 6.0 (Media Cybernetics, Bethesda, MA, USA).

2.9 Quantitative Reverse Transcription Polymerase Chain Reaction (qRT-PCR)

Total RNA was extracted from tumor and lung tissue using the mirVana™ RNA Isolation Kit (Invitrogen, Carlsbad, USA, AM1561) and then subjected to cDNA synthesis with RevertAid First Strand cDNA Synthesis kit (Thermo Scientific, Waltham MA, USA,K1622) in a PCR instrument (C1000 Touch Thermal

Cycler, Bio-Rad, CA, USA). The q-PCR quantitation was performed using ABI 7900HT Real-time PCR System (Applied Biosystems, Waltham, USA). The q-PCR amplification cycling protocol was as follows: 95°C for 5 min, followed by 40 cycles of 95°C for 10 s and 60°C for 30s. Each sample was analyzed in triplicate. The primer sequences shown in Table 2 were designed by Shanghai Generay Biotech Co., Ltd. (Shanghai, China). The target mRNA expression levels were normalized based on the level of the reference gene β-actin, and then the results were calculated using the $2^{-\Delta\Delta Ct}$ method.

Table-2 Primer sequences uesed in this study

Target gene	Forward primer (5'-3')	Reverse primer (5'-3')
E-Cadherin	AACGCTCCTGTCTTCAACCC	GGGCATCATCATCGGTCACT
Vimentin	GGTTGAGACCAGAGATGGACAG	GTCTTTTGGGGTGTCAGTTGTTA
Snail	AGATGCACATCCGAAGCCAC	GGTCAGCAAAAGCACGGTTG
MMP-9	GCAGAGGCATACTTGTACCG	TGATGTTATGATGGTCCCACTTG
β-actin	GTCGT ACCAC AGGCA TTGTG ATGG	GCAAT GCCTG GGTAC ATGGT GG

2.10 Western Blot Analysis

BC tissue and lung tissue from experimental mice were homogenized in ice-cold RIPA buffer containing protease inhibitors, and the protein-containing supernatants were separated and collected by centrifugation at 10,000 rpm at 4°C for 15 min. Protein concentrations were determined using a bicinchoninic acid kit (Thermo Scientific, Waltham, USA) with bovine serum albumin as a standard. Equivalentamounts of protein from each sample were separated by 10% SDS–PAGE and transferred onto polyvinylidene difluoride membranes. After blocking with 5% defatted milk, the membranes were incubated with primary antibodies overnight at 4°C and then incubated with HRP-conjugated secondary antibodies. The primary antibodies included rabbit anti-E-cadherin (ab8978, abcam,1:10000), mouse anti-Vimentin (ab40772, abcam, 1:1000), rabbit anti-MMP-9 (ab76003, abcam,1:5000), rabbit anti-Snail (ab216347, abcam,1:1000), rabbit anti-Bcl-2 (ab32124, abcam,1:1000), rabbit Anti-Cleaved Caspase-3 (ab32042, abcam,1:500). The signals were detected with an enhanced chemiluminescence reagent (Thermo Scientific, Waltham, USA). The bands were analyzed via densitometry using Image Lab (Bio-Rad, California, USA) and standardized to b-actin and were expressed as fold changes relative to the control value.

2.11 Statistical analysis

All data are presented as the mean ± SEM and analyzed by analysis of variance. The differences between two groups were analyzed by an unpaired Student's t-test using GraphPad PRISM statistical software package version 8.0 for Windows (GraphPad Software, San Diego, CA USA) ,and $P < 0.05$ was considered as statistically significant.

3. Results

3.1. Identification of the Main Components of JPTQ Decoction

The JPTQ Decoction is an improved formula of the classic formula "Si Jun Zi Decoction". Some studies have confirmed the therapeutic effect of Sijunzi Decoction in tumor diseases[36, 37]. Its clinical application has obviously improved the quality of life of BC patients, prolonged the survival time of patients, and reduced the incidence of lung metastases. Before further exploring the mechanism of JPTQ decoction, we preliminarily identified the main components of JPTQ decoction by HPLC-MS. Fig. 1A shows the (Electrospray ionization, ESI)(+) mode and ESI(-) mode total ion chromatogram (TIC) respectively.

In the secondary mass spectrum analysis table of JPTQ decoction, the relative content of a compound was judged based on the matching degree of multiple databases greater than 80 and the peak area size, and the top 12 compounds (Table-3) with different content abundance under different modes were selected (Fig. 1B). These compounds are shown in Table-3. Although JPTQ has not traditionally been used to treat BC, some of its active compounds, such as resveratrol [30], genistein [31], galangin [32], and quinic acid [33], have been shown to have effective anti-tumor and anti-metastatic effects in different models. These anti-cancer compounds become the material basis for the effectiveness of the formula.

Table 3 JPTQ decoction Mass Spectrometry compounds identification
(Top 12, sorted by relative abundance)

No.	Name	Structure	Formula	retention time (min)	Area	Molecular weight (Da)
1	Resveratrol		C14 H12 O3	8.88	1.67E+08	228.078
2	DL-Arginine		C6H14N4O2	0.442	1.55E+08	174.11131
3	Genistin		C21 H20 O10	12.737	1.24E+08	432.105
4	Genistein		C15 H10 O5	16.26	9.34E+07	270.0527
5	Boldenone undecylenate		C30 H44 O3	15.897	8.54E+07	452.3276
6	D-(-)-Quinic acid		C7 H12 O6	0.522	7.84E+07	210.073
7	Proline	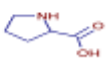	C5 H9 N O2	0.506	6.96E+07	115.0634
8	Chlorogenic acid		C16 H18 O9	6.722	4.13E+07	354.0948
9	Eplerenone		C24 H30 O6	15.007	3.40E+07	414.20305
10	L-Pyroglutamic acid		C5 H7 N O3	0.951	3.08E+07	129.04251
11	Neochlorogenic acid		C16 H18 O9	7.165	2.52E+07	354.09489
12	Ageratriol		C15 H24 O3	13.357	2.47E+07	234.16126

3.2. JPTQ Decoction Retard the Proliferation of in-situ Tumor and Promoted its Necrosis and Apoptosis

On the day of starting the JPTQ intervention (Day 0), baseline Biofluorescence values were measured between the two groups (Fig. 2A), and no statistical difference was found (*P*=0.34, Fig. 2D).

After two weeks of JPTQ decoction intervention, biofluorescence imaging (Fig. 2B) was performed again. The biofluorescence value of mice in the JPTQ group was weaker than that in the model group, but there was no statistical difference (*P*=0.4706) (Fig. 2E). The 3rd biofluorescence imaging (Fig. 2C) was evaluated again at the end of the experiment (4 weeks). The biofluorescence value of the JPTQ group was significantly weaker than that of the model group, with a statistical difference (Fig. 2F, P=0.049). We measured the tumor volume and body weight changes of tumor-bearing mice per three days. Within 4 weeks of drug intervention, the tumor volume of JPTQ group was smaller than that of the model group

(Fig. 2G). Till the end of the experiment, the mean tumor volume and weight of JPTQ group was still smaller than that of the model group (Fig. 2I,J), on the 28th day of sacrifice, although it was not as different as the bioluminescence value at the end of the experiment (Fig. 2H, P=0.3045). The weight change curves of the two groups were also measured and recorded per three days. In the experiment, with the extension of tumor bearing time, the weight of mice in both groups decreased, but the weight loss rate of mice in the model group was significantly higher than that in the JPTQ group (Fig. 2K). At the end of the fourth week, the weight of mice in the JPTQ group was significantly higher than that in the model group (Fig. 2M) (P=0.0313). Excessive splenomegaly indicates that it has entered the stage of negative immune regulation, which is closely related to tumor immune escape [38]. The spleen weight of JPTQ group decreased significantly (Fig. 2L) (P=0.0333). Compared with the model group, the tumor tissue in JPTQ group had less inflammatory infiltration and more necrosis (Fig. 2N).

we also studied the anti-proliferation and anti-angiogenesis effects of JPTQ. The expression of proliferation protein Ki-67 and angiogenesis marker VEGF protein in tumor samples of TNBC bearing mice was studied by IHC assay. In the JPTQ group, the expression of Ki-67 and VEGF were significantly lower than that in the model group (Fig. 2O,P, P<0.0001, P=0.0139). For verify the pro-apoptotic effect of JPTQ, we studied the expression levels of pro-apoptotic protein cleved-caspase 3 and anti-apoptotic protein Bcl-2 in tumor tissues. The expression of cleved-caspase 3 of JPTQ group was significantly increased compared with that in the model group (Fig. 2Q, P=0.0489), while the expression of Bcl-2 was significantly decreased (Fig. 2R, P=0.1275). These results were consistent with the results of transcriptome analysis, indicating that the apoptotic pathway is one of the pathways of the therapeutic effect of JPTQ decoction.

3.3. JPTQ Decoction Significantly Reduced Lung Metastasis in TNBC Bearing Mice

4T1 BC cells is TNBC cell lines with high metastatic characteristics [38–40]. The isolated lung tissue biofluorescence imaging results were as follows Fig. 3A, 6 mice in the model group had different degrees of lung metastasis, and only one mice in the JPTQ group had slightly lung metastasis. The statistical analysis of biofluorescence imaging values of the two groups showed that there was significant difference between the two groups (Fig. 3B, P=0.0476), compared with JPTQ group, the model group has higher biofluorescence value, which means more serious lung metastasis.

The HE pathological analysis of lung tissue also found that the model group had larger tumor infiltration area and more metastatic lesions (Fig. 3D,E). In Fig. 3D, extensive alveolar wall thickening was found in the lung tissue of the model group, accompanied by a large number of lymphocytes and neutrophils infiltration (black arrow), a large number of tumor cells (green arrow) were found in the tissue, bleeding can be seen around the local blood vessels (yellow arrow). In Fig. 3E, in JPTQ group, the thickening of alveolar wall was improved, and the infiltration of lymphocytes and neutrophils was decreased (black arrow),a small amount of tumor cell mass (green arrow) was found in the tissue, local perivascular bleeding decreased (yellow arrow). After sacrificing mice, there was no statistically significant difference

in lung tissue weighing between the two groups, but the mean lung weight of the JPTQ group was lower than that of the model group (Fig. 3C, P=0.5637), which was considered to be because the model group had more severe tumor load accompanied by inflammatory infiltration and edema.

We also analyzed whether the reduction of lung metastasis is related to the inhibition of proliferation and promotion of apoptosis. WB analysis showed that the expression of cleaved caspase-3 was significantly increased (Fig. 3F, P=0.0428) and the expression of Bcl-2 was significantly decreased (Fig. 3G, P=0.0168) in pulmonary metastases of JPTQ group. In addition, immunohistochemical analysis revealed that the expression of Ki-67 and VEGF in JPTQ group was significantly decreased compared with model group (Fig. 3H,I, P<0.0001, *P*=0.0170 respectively).

3.4. Transcriptome Analysis of Tumor Tissue and Lung Tissue in Tumor Bearing Mice

For explore the specific mechanism of JPTQ decoction in reducing tumor proliferation and progression and lung metastasis, we sequenced the transcriptome of lung and tumor tissue of two groups of mice. A total of 191 differentially expressed Genes (DEGs) were screened out in tumor tissues, including 163 up-regulated genes and 28 down-regulated genes (Fig. 4A).

KEGG pathway analysis indicated the PI3K-Akt, PPAR, Estrogen signaling pathway, ECM-receptor interaction and other pathways were significantly enriched (Fig. 4B).The Gene Ontology (GO) analysis revealed obvious enrichment of immune-related functions in biological processes (BP) category, such as immune response, immunoglobulin generation, and B cell receptor signaling pathway (*P*<0.05 respectively) (Fig. 4C). In the cellular component (CC) category, the greatest numbers of genes were found in the “Extracellular regions” and “extracellular matrix”(*P*<0.05 respectively) (Fig. 4D). In the molecular function (MF) category, the“Protein binding”(Fig. 4E) was regulated signifcantly(*P*<0.05).

A total of 207 differentially expressed genes were identified in lung tissues, including 98 up-regulated genes and 109 down regulated genes (Fig. 4F). KEGG pathway analysis showed that adhesion plaque, chemokine signaling pathway, IL-17 signaling pathway, etc. were significantly enriched (Fig. 4G, P<0.05 respectively). The Go analysis was also performed, in the category of BP, inflammation, immune function, etc. were significantly enriched (Fig. 4H). In the MF category, the “ Integrin, Chemokine Activation, EGFR Binding, FATZ binding, etc. (Fig. 4J) was regulated signifcantly (*P*<0.05). In the CC category, focal adhesion, etc. were significantly enriched (Fig. 4I).

EMT process changes, angiogenesis, EGFR overexpression and other mechanisms will also aggravate the malignant phenotype of BC. RNA sequencing of tumor bearing lung tissue and tumor tissue indicated that EMT process related genes, proliferation, anti apoptosis related genes and angiogenesis related genes were down regulated (See Supplementary Tables S1and S2).

3.5. JPTQ Significantly Improved the Tumor Immune Microenvironment of Tumor Bearing Mice

The escape of tumor immune to aggravate the occurrence and development of tumor diseases [41]. The transcriptome analysis of lung and tumor tissues indicated that the pathways or biological processes related to immune function were significantly enriched. So,we analyzed the changes in the immune microenvironment of the experimental mice by FCM. We analyzed the of overall immune status of tumor-bearing mice, that is, the proportion of $CD4^+$ T cells in the peripheral blood, $CD4^+$ T cells in mice in the JPTQ treatment group were significantly increased, compared with the model group (40.95% VS 55.83%, Fig. 5A,B, P=0.0384). On the basis of these findings, we further analyzed the difference of the effector Th1/2 cells in the spleen of two groups of tumor-bearing mice, and the FCM analysis results indicated that although no difference was observed in the proportion of Th2 cells between the two groups (0.7% VS 0.93%, *P*=0.0572, Fig. 5E), but the Th1 cells were significantly increased in the JPTQ group,compared with the model group (2.333% VS 1.167% *P*=0.0095, Fig. 5D). The imbalance of Th1/2 cells was improved to some extent (Fig. 5C).

Treatment with JPTQ also reduced the incidence of lung metastasis in tumor-bearing mice, so we also analyzed the local immune microenvironment in the lung. The MDSCs is divided into M-MDSCs and PMN-MDSCs. The two cell subsets perform different immunosuppressive functions [22, 23]. By FCM analysis, it was found that the proportion of M-MDSC in the lung single cell suspension of mice in the model and JPTQ group were 2.602% and 1.911% respectively (Fig. 5F), The lung M-MDSC in the mice of JPTQ group was significantly reduced (Fig. 5G, P=0.001). The proportion of PMN-MDSC in single-cell lung suspension in the model group and the JPTQ group was 14.70% (Fig. 5F) and 18.64% respectively(Fig. 5F), and no difference was observed between the two groups (Fig. 5H, P=0.2834).

3.6. JPTQ Decoction Reduced the Tumor Proliferation and Occurrence of Lung Metastasis in Tumor-Bearing Mice by Regulating the EMT Process

EMT is the key link of malignant transformation of many tumor diseases, which can promote the occurrence, proliferation and distant metastasis of tumor. Transcriptome analysis of tumor samples showed that EMT related genes such as E-cadherin were up-regulated, snail was down regulated, but Vimentin and MMP-9 were not changed (See Supplementary Tables S1 and S2).

The q-PCR was used to verify the results of transcriptomics.In tumor tissues, the results showed that E-cadherin, Vimentin and MMP9 expression was up-regulated (Fig. 6A,B,D, P=0.001, *P*=0.0002 and *P*=0.0127 respectively), Snail expression was down regulated (Fig. 6C, P□0.0001).

The results of IHC showed that E-cadherin was significantly increased in JPTQ group (Fig. 6I, P=0.0403, Fig. 6Q), Vimentin and MMP-9 was not significantly different between the two groups (Fig. 6J,Q, P=0.698; Fig. 6L,Q, P=0.568), Snail was significantly decreased in JPTQ group (Fig. 6K, P=0.0371, Fig. 6Q). WB was used to detect EMT-associated proteins expression status (Fig. 6S, Fig. 6U). WB results of tumor tissue showed that the expression of E-cadherin in the JPTQ group was significantly higher than that in the model group (*P*=0.0196), and Vimentin had no significant difference between the two groups (*P*=0.1917), but there was a down-trend in JPTQ group. Snail was significantly down regulated in JPTQ

group (*P*=0.0463), and MMP-9 showed a downward trend, but there was no statistical significance (*P*=0.3152). The q-PCR revalidation, WB, and immunohistochemical results were basically the same as transcriptome results. Combined with the above conclusions, we can conclude that the inhibition of JPTQ decoction on the proliferation of in-situ tumors may be partly due to the regulation of EMT process.

Transcriptome analysis of lung tissue in JPTQ group showed that the expressions of EMT related genes such as E-cadherin, Snail and MMP-9 were higher than those in model group, while Snail expression was lower than that in model group (supplementary material). q-PCR results showed that compared with the model group, the expression of E-cadherin and Vimentin increased (Fig. 6E, F *P*=0.0303, *P*□0.0001), snail and MMP-9 decreased (Fig. 6G, H, P=0.0001, *P*=0.0003) in JPTQ group. The results of IHC showed that E-cadherin in JPTQ group was significantly higher than that in model group (Fig. 6M, P=0.004, Fig. 6R), and Vimentin in JPTQ group was not different from that in model group (Fig. 6N, P=0.3039, Fig. 6R). MMP-9 and Snail was significantly down regulated (Fig. 6O,P, P=0.038, *P*=0.0471, Fig. 6R). In the WB results of lung tissue(Fig. 6T), E-cadherin was significantly increased in the JPTQ group compared with the model group (Fig. 6V, P=0.0492), while Vimentin was insignificant in the two groups (Fig. 6V, P=0.2120), but the JPTQ group showed a decreasing trend. Snail and MMP-9 were significantly down-regulated in the JPTQ group (Fig. 6V, P=0.0299, *P*=0.0273). Combined with the results of IHC and WB, it was considered that MMP-9 showed a down-trend in the lung tissue of mice in the JPTQ group. As mentioned above, JPTQ realizes the regulation of EMT process through the regulation of targets such as E-cadherin, Snail and MMP-9, thereby reducing the occurrence of lung metastasis.

4. Discussion

The TCM has accumulated rich practical experience in the diagnosis and treatment of cancer diseases, and played an impressive role in enhancing efficacy and reducing toxicity, improving quality of life and even directly treating cancer among cancer patients. The JPTQ decoction used in this study is an improved formula of Si-Jun-Zi decoction, which is a classic formula from the Song Dynasty "Taiping Huimin He Ji Ju Fang", and has been used for more than 900 years. On the basis of the clinical changes and clinical symptoms of BC patients, our research team improved it by adding Radix Curcumae Aromaticae, Lophatherum gracile and Fructus Akebiae. In clinical application, JPTQ decoction has improved the discomfort reaction of patients during the treatment of radiotherapy and chemotherapy, improved the quality of life, and reduced the occurrence of lung metastasis of BC. In order to analyze the mechanism, our research team conducted this study. In the HPLC-MS analysis of the JPTQ decoction, according to the size of their peak area [42, 43], the top 12 components were included in analysis.Many related studies have confirmed their anti-tumor activity in these components. Because of this, the JPTQ decoction has the basis for anti-tumor and anti-metastatic effects.

BC progression is associated with several hallmark events of cancer, such as loss of epithelial differentiation, angiogenesis, immunosuppression, and uncontrolled proliferation and escape from apoptotic responses [44]. Our study confirms the above effect of JPTQ. After successfully modeling animal model of BC, we evaluated the anti-tumor efficacy of JPTQ decoction. There is no difference in the

baseline and midterm evaluation of biofluorescence imaging of tumor-bearing mice, but a downward trend is observed. After 28 days of JPTQ intervention, the biofluorescence values of tumors and lung metastases in the JPTQ group were lower than those in the model group, showing statistics Significantly, the HE pathological analysis also showed that the tumor samples in the JPTQ group had more necrotic areas than the model group. The tumor volume growth curve showed that the tumor volume growth of the JPTQ group was significantly slower than that of the model group. In addition, JPTQ decoction also has a definite effect on maintaining the body weight of tumor-bearing mice, the observation of the weight growth curve showed that, and the body weight of mice in the model group was significantly lower than that in the JPTQ group at the end of the experiment. The body weight of all the tumor-bearing mice showed a decreasing trend during the experimental observation period, but the decreasing trend of the tumor-bearing mice in the JPTQ group was slower than that in the model group. In tumor-bearing animals, the spleen is often compensatory enlargement, suggesting the state of immunodeficiency. After sacrificing mice, the comparison of the spleen weight of the two groups of experimental mice showed that the spleen weight of the mice in the JPTQ group was significantly reduced, indicating that the immune state of the tumor-bearing mice was improved to a certain extent. Therefore, it is believed that JPTQ decoction can inhibit the proliferation of BC to a certain extent, and can improve the body weight and other general states of tumor-bearing mice.

Metastasis of distant organs is an important factor in the failure of BC treatment [45]. The bioluminescence imaging observation of experimental mice showed that the fluorescence value of lung metastasis in the JPTQ group was significantly lower than that in the model group, all the 6 mice in the model group had lung metastasis, while only one mice in the JPTQ group.HE pathological analysis of lung tissue also showed that the model group had larger tumor area and more metastatic lesions in the lungs or tumor samples than the JPTQ group, and the alveolar wall thickening, lymphocyte and neutrophils infiltration, and perivascular bleeding were also more serious than those in the JPTQ group. Lung tissue weighing showed no statistical difference between the two groups, but the mean lung weight of mice in the JPTQ group was lower than that in the model group, considering that the mice in the model group had more severe tumor load accompanied by inflammatory infiltration and edema.

In order to explore the specific mechanism of JPTQ decoction in inhibiting tumor proliferation and progression and lung metastasis, transcriptome analysis was performed on the lung tissues and tumor tissues of the two groups of mice. The GO analysis of differential genes in tumor tissue showed that immune response, B cell receptor signaling pathway and so on of immune-related functions were significantly enriched. The GO analysis of DEGs in lung tissue showed significant enrichment of biological processes such as inflammation, immune function,etc. From the transcriptome results, it is not difficult to see that immune-related pathways or biological processes are significantly enriched in the lung tissues and tumor tissues of mice in the JPTQ group, revealing its effect on immune regulation. The immune state of the body is directly related to the occurrence and development of tumors. Based on transcriptome analysis, we assessed the differences in immune status between the two groups of tumor-bearing mice. Th1, Th2 and Th17 are the main types of T helper cells, which belong to subgroup of $CD4^+$

T cells [46]. We first found that the peripheral blood $CD4^+$T cells in the JPTQ group were significantly increased, so next we analyzed the changes of Th1/2 cells in the spleen, the largest peripheral immune organ. The results indicated that the Th1 cells of mice in JPTQ group were significantly increased. IFN-γ secreted by $CD4^+$ T cells has a powerful antitumor effect and reduces the infiltration and polarization of immunosuppressive cells [30]. JPTQ treatment also reduced the incidence of lung metastasis in tumor-bearing mice, so we also analyzed changes in the local immune microenvironment in the lung. MDSC is a population of immunosuppressive cells [22], we analyzed the relationship between the decrease of lung metastasis and MDSCs in lung local TIME. It was found that the proportion of M-MDSC in the mice lung in the JPTQ group was significantly lower than that in the model group (1.911% VS 2.602%), and no difference was observed in PMN-MDSC. Due to the short survival period of PMN-MDSC, current research on the differentiation of MDSC is mainly based on M-MDSC, which can migrate to tumor foci and differentiate into tumor-associated macrophages (TAMs) [47]. In addition, Haverkamp et al. found that M-MDSCs mediated sustained inhibition of T cell function in tumor mouse models, whereas PMN-MDSCs did not [48]. Therefore, we can assume that the mice in the JPTQ group, the lung immunosuppressive MDSC is significantly reduced, which is easier to exert the immune cell effect. Therefore, mice with JPTQ decoction intervention have a lower lung metastasis rate.

In addition, mechanisms such as altered EMT process, angiogenesis, and high expression of anti-apoptotic factors can also aggravate the malignant phenotype of BC. The change of EMT process is the most classical metastasis pathway. The EMT regulatory factors include E-cadherin, Vimentin, MMP-9, Snail, etc. MMP-9 degrade a range of ECM proteins and have a profound impact on cancer progression by affecting angiogenesis, invasion, and migration [49]. Vimentin regulates the interaction between cytoskeletal proteins, cell adhesion molecules and other proteins. Cancer cells with high expression have high invasion and migration ability [50]. E-catherin keeps the cancer cells in close contact with each other, making it difficult to separate from the primary tumor, thus inhibiting invasion and metastasis of tumor [51]. Snail is the first and most important E-adhering transcriptional inhibitor, and it is closely related to metastasis, recurrence and poor prognosis of BC [52]. RNA sequencing of lung tissues and tumor tissues in JPTQ group showed down-regulation of EMT process related genes, proliferation and anti-apoptosis related genes, and angiogenesis related genes. The q-PCR, WB and IHC results indicated that E-cadherin in the tumor and lung tissue of mice in the JPTQ group was increased, while Snail was down-regulated. MMP-9 was also observed to be down-regulated in lung tissue. Apoptosis is also a hallmark event of limited tumor proliferation [16]. In JPTQ group, the pro-apoptotic protein cleaved caspase 3 was up-regulated and the anti-apoptotic protein Bcl-2 was down regulated. Uncontrolled tumor cell proliferation is a feature of most cancers [12]. Therefore, we detected the cell proliferation marker Ki67 to analyze the anti-proliferation effect of JPTQ on in-situ tumors. The results of immunohistochemistry showed that Ki67 in tumor and lung metastasis microenvironment was significantly down regulated in a group of mice treated with JPTQ, suggesting that JPTQ decoction can inhibit the progression of tumor and lung metastasis by inhibiting tumor proliferation. Angiogenesis is a basic biological feature of tumors, so it is an effective treatment strategy to inhibit tumor growth by interfering with the binding of VEGF to VEGFR

[15]. The expression of VEGF was down-regulated in lung tissues and tumor tissues of mice in the JPTQ group, indicating that the angiogenesis associated with tumor proliferation was significantly reduced.

To sum up, JPTQ decoction improved the immunosuppressive microenvironment of tumor-bearing mice, reduced the number of M-MDSCs, increased the proportion of effector Th1 cells, and enhanced the recognition and killing effect of immune cells.In addition, JPTQ also reverses the EMT process and reduces angiogenesis-related factors. Therefore, tumor angiogenesis is reduced, and sufficient nutritional support is not available. Tumor cells face great survival pressure, proliferation is inhibited, and apoptosis increases accordingly. These mechanisms do not work in isolation, but complement each other to form a network of interactions that ultimately shrink tumors and reduce lung metastases in tumor-bearing mice.

5. Conclusions

JPTQ decoction has a certain inhibitory effect on the TNBC, and significantly reduces the incidence of lung metastasis. Its effect depends mainly on improving the negative immune microenvironment, inhibiting proliferation and tumor angiogenesis, promoting tumor apoptosis, and regulating the EMT process.

Abbreviations

BC: breast cancer; **BP:**biological processes ;**CC:**cellular component**DEGs:**differentially expressed genes **EMT:** epithelial to mesenchymal transition**ESI:**electrospray ionization**FCM:**flow cytometry**GO:** gene ontology**HE:**hematoxylin and eosin**HPLC-MS:**high performance liquid chromatography and mass spectrometry**IFNγ:**interferon-γ**IHC:**immunohistochemistry**IL-4:**secrete Interleukin 4**JPTQ:**jianpitiaoqi decoction**KEGG:**kyoto encyclopedia of genes and genomes**MDSCs:**myeloid derived suppressor cells **MF:**molecular function**M-MDSCs:** monocytes-MDSCs**MMP-9:**matrix metalloprotein-9**PMN-MDSCs:** polymorphonuclear-MDSCs**qRT-PCR:** quantitative real time polymerase chain reaction**SEM:** standard error of mean**TCM:**traditionalchinese medicine**Th1/2**:T helper 1/2 cell**TIC:** total ion chromatogram **TIME:**tumor immune microenvironment**TNBC:** triple negative breast cancer**VEGF:**vascular endothelial growth factor**WB:**western blot.

Declarations

Acknowledgements

Not applicable.

Authors' contribution

Yong Guo, Qinghua Yao conceived the research;

Jin Zhang, Biyu Cai, Chenxiao Ye, Haitao Chen, Xinrong Li, Zhili Xu performed the experiments;

Jin Zhang, Yi Lu, Chenxiao Ye wrote the manuscript; all authors reviewed the manuscript.

Funding

The study was supported by The National Natural Science Foundation of China (Nos.81973805) and Thechinese medicine reserch program of Zhejiang Province (No. 2020ZA018).

Availability of data and materials

The data analyzed during this study can be obtained from the corresponding

author on reasonable request.

Conflicts of Interest

The authors have declared no conflicts of interest.

All authors agree to publish this article.

Ethics approval

All animal experiments were approved by the experimental animal ethics committee of Zhejiang Chinese Medical University.

Consent for publication

All authors agree to publish this article.

References

1. Sung H, Ferlay J, Siegel RL, Laversanne M, Soerjomataram I, Jemal A, Bray F: Global Cancer Statistics 2020: GLOBOCAN Estimates of Incidence and Mortality Worldwide for 36 Cancers in 185 Countries. CA Cancer J Clin2021, 71(3):209-249.
2. Wahba HA, El-Hadaad HA: Current approaches in treatment of triple-negative breast cancer. Cancer Biol Med2015, 12(2):106-116.
3. Peddi PF, Ellis MJ, Ma C: Molecular basis of triple negative breast cancer and implications for therapy. Int J Breast Cancer2012, 2012:217185.
4. Tarin D, Matsumura Y: Recent advances in the study of tumour invasion and metastasis. J Clin Pathol1994, 47(5):385-390.
5. Fidler IJ: The organ microenvironment and cancer metastasis. Differentiation2002, 70(9-10):498-505.
6. Singh A, Settleman J: EMT, cancer stem cells and drug resistance: an emerging axis of evil in the war on cancer. Oncogene2010, 29(34):4741-4751.

7. Gavert N, Ben-Ze'ev A: Epithelial-mesenchymal transition and the invasive potential of tumors. Trends Mol Med2008, 14(5):199-209.
8. Liu R, Zheng HG, Li WD *et al*: Anti-tumor enhancement of Fei-Liu-Ping ointment in combination with celecoxib via cyclooxygenase-2-mediated lung metastatic inflammatory microenvironment in Lewis lung carcinoma xenograft mouse model. J Transl Med2015, 13.
9. Stetler-Stevenson WG: The Role of Matrix Metalloproteinases in Tumor Invasion, Metastasis, and Angiogenesis. Surgical Oncology Clinics of North America2001, 10(2):383-392.
10. Kang E, Seo J, Yoon H, Cho S: The Post-Translational Regulation of Epithelial-Mesenchymal Transition-Inducing Transcription Factors in Cancer Metastasis. Int J Mol Sci2021, 22(7).
11. Yang ZJ, Zhang B, Liu BW, Xie YG, Cao XC: Combined Runx2 and Snail overexpression is associated with a poor prognosis in breast cancer. Tumor Biol2015, 36(6):4565-4573.
12. Giridhar KV, Liu MC: Available and emerging molecular markers in the clinical management of breast cancer. Expert Rev Mol Diagn2019, 19(10):919-928.
13. Sykaras AG, Pergaris A, Theocharis S: Challenging, Accurate and Feasible: CAF-1 as a Tumour Proliferation Marker of Diagnostic and Prognostic Value. Cancers2021, 13(11).
14. Chong ZX, Yeap SK, Ho WY: Angiogenesis regulation by microRNAs and long non-coding RNAs in human breast cancer. Pathol Res Pract2021, 219:153326.
15. Chen PC, Chen CC, Ker YB, Chang CH, Chyau CC, Hu ML: Anti-Metastatic Effects of Antrodan with and without Cisplatin on Lewis Lung Carcinomas in a Mouse Xenograft Model. International Journal of Molecular Sciences2018, 19(6).
16. Cao Y, Di X, Zhang Q, Li R, Wang K: RBM10 Regulates Tumor Apoptosis, Proliferation, and Metastasis. Front Oncol2021, 11:603932.
17. Xie Y, Akpinarli A, Maris C, Hipkiss EL, Lane M, Kwon EK, Muranski P, Restifo NP, Antony PA: Naive tumor-specific CD4(+) T cells differentiated in vivo eradicate established melanoma. J Exp Med2010, 207(3):651-667.
18. Quezada SA, Simpson TR, Peggs KS *et al*: Tumor-reactive CD4(+) T cells develop cytotoxic activity and eradicate large established melanoma after transfer into lymphopenic hosts. J Exp Med2010, 207(3):637-650.
19. Mantovani A, Allavena P, Sica A, Balkwill F: Cancer-related inflammation. Nature2008, 454(7203):436-444.
20. Maier E, Duschl A, Horejs-Hoeck J: STAT6-dependent and -independent mechanisms in Th2 polarization. Eur J Immunol2012, 42(11):2827-2833.
21. Kumar V, Patel S, Tcyganov E, Gabrilovich DI: The Nature of Myeloid-Derived Suppressor Cells in the Tumor Microenvironment. Trends Immunol2016, 37(3):208-220.
22. Bronte V, Brandau S, Chen SH *et al*: Recommendations for myeloid-derived suppressor cell nomenclature and characterization standards. Nat Commun2016, 7:12150.

23. Wang PF, Song SY, Wang TJ, Ji WJ, Li SW, Liu N, Yan CX: Prognostic role of pretreatment circulating MDSCs in patients with solid malignancies: A meta-analysis of 40 studies. Oncoimmunology2018, 7(10):e1494113.
24. De Sanctis F, Solito S, Ugel S, Molon B, Bronte V, Marigo I: MDSCs in cancer: Conceiving new prognostic and therapeutic targets. Biochim Biophys Acta2016, 1865(1):35-48.
25. Bodai BI, Tuso P: Breast cancer survivorship: a comprehensive review of long-term medical issues and lifestyle recommendations. Perm J2015, 19(2):48-79.
26. Emens LA: Breast Cancer Immunotherapy: Facts and Hopes. Clin Cancer Res2018, 24(3):511-520.
27. Cardoso F, Harbeck N, Barrios CH *et al*: Research needs in breast cancer. Ann Oncol2017, 28(2):208-217.
28. Tian X, Liu L: Effect and advantage of orally taking Chinese herbal medicine for treatment of lung cancer]. Zhongguo Zhong Yao Za Zhi2010, 35(21):2795-2800.
29. Qiu X, Jia J: Research advances on TCM anti-tumor effects and the molecular mechanisms. J Cancer Res Ther2014, 10 Suppl 1:8-13.
30. Chen L, Musa AE: Boosting immune system against cancer by resveratrol. Phytother Res2021, 35(10):5514-5526.
31. Zhang HY, Cui J, Zhang Y, Wang ZL, Chong T, Wang ZM: Isoflavones and Prostate Cancer: A Review of Some Critical Issues. Chin Med J (Engl)2016, 129(3):341-347.
32. Fang D, Xiong Z, Xu J, Yin J, Luo R: Chemopreventive mechanisms of galangin against hepatocellular carcinoma: A review. Biomed Pharmacother2019, 109:2054-2061.
33. Baraya YS, Wong KK, Yaacob NS: The Immunomodulatory Potential of Selected Bioactive Plant-Based Compounds in Breast Cancer: A Review. Anticancer Agents Med Chem2017, 17(6):770-783.
34. Chen Q: **Pharmacological experimental methods of traditional Chinese medicine**. Beijing: People's Health Publishing House; 1994.
35. Yoshimura K, Hazama S, Iizuka N, Yoshino S, Yamamoto K, Muraguchi M, Ohmoto Y, Noma T, Oka M: Successful immunogene therapy using colon cancer cells (colon 26) transfected with plasmid vector containing mature interleukin-18 cDNA and the Igkappa leader sequence. Cancer Gene Ther2001, 8(1):9-16.
36. Gan D, Xu A, Du H, Ye Y: Chinese Classical Formula Sijunzi Decoction and Chronic Atrophic Gastritis: Evidence for Treatment Approach? Evid Based Complement Alternat Med2017, 2017:9012929.
37. Chen JM, Yang TT, Cheng TS *et al*: Modified Sijunzi decoction can alleviate cisplatin-induced toxicity and prolong the survival time of cachectic mice by recovering muscle atrophy. J Ethnopharmacol2019, 233:47-55.
38. Brar SS, Seevaratnam R, Cardoso R, Law C, Helyer L, Coburn N: A systematic review of spleen and pancreas preservation in extended lymphadenectomy for gastric cancer. Gastric Cancer2012, 15 Suppl 1:S89-99.

39. Pulaski BA, Ostrand-Rosenberg S: Mouse 4T1 breast tumor model. Curr Protoc Immunol2001, Chapter 20:Unit 20 22.
40. Yang S, Zhang JJ, Huang XY: Mouse models for tumor metastasis. Methods Mol Biol2012, 928:221-228.
41. Cao X: Immunological problems in tumor growth and metastasis. Chinese Journal of tumor biotherapy2007, 14(001):2-6.
42. Wu N: Calculation of chromatographic peak area. Analytical chemistry, 5(3):243-245.
43. Geng W: Comparative analysis of fatty acid content in papaya seeds by external standard method and peak area normalization method. Chemical engineer2015, 29(1):23-24.
44. Rojo de la Vega M, Chapman E, Zhang DD: NRF2 and the Hallmarks of Cancer. Cancer Cell2018, 34(1):21-43.
45. Park H, Chang SK, Kim JY, Lee BM, Shin HS: Risk factors for distant metastasis as a primary site of treatment failure in early-stage breast cancer. Chonnam Med J2014, 50(3):96-101.
46. Ahrends T, Spanjaard A, Pilzecker B, Babala N, Bovens A, Xiao Y, Jacobs H, Borst J: CD4(+) T Cell Help Confers a Cytotoxic T Cell Effector Program Including Coinhibitory Receptor Downregulation and Increased Tissue Invasiveness. Immunity2017, 47(5):848-861 e845.
47. Shand FH, Ueha S, Otsuji M *et al*: Tracking of intertissue migration reveals the origins of tumor-infiltrating monocytes. Proc Natl Acad Sci U S A2014, 111(21):7771-7776.
48. Haverkamp JM, Smith AM, Weinlich R *et al*: Myeloid-derived suppressor activity is mediated by monocytic lineages maintained by continuous inhibition of extrinsic and intrinsic death pathways. Immunity2014, 41(6):947-959.
49. Han YH, Kee JY, Kim DS, Mun JG, Park SH, Kim YJ, Um JY, Hong SH: Arctii Fructus Inhibits Colorectal Cancer Cell Proliferation and MMPs Mediated Invasion via AMPK. Am J Chin Med2017, 45(6):1309-1325.
50. McInroy L, Maatta A: Down-regulation of vimentin expression inhibits carcinoma cell migration and adhesion. Biochem Biophys Res Commun2007, 360(1):109-114.
51. Ray ME, Mehra R, Sandler HM, Daignault S, Shah RB: E-cadherin protein expression predicts prostate cancer salvage radiotherapy outcomes. J Urol2006, 176(4 Pt 1):1409-1414; discussion 1414.
52. Moody SE, Perez D, Pan TC, Sarkisian CJ, Portocarrero CP, Sterner CJ, Notorfrancesco KL, Cardiff RD, Chodosh LA: The transcriptional repressor Snail promotes mammary tumor recurrence. Cancer Cell2005, 8(3):197-209.

Figures

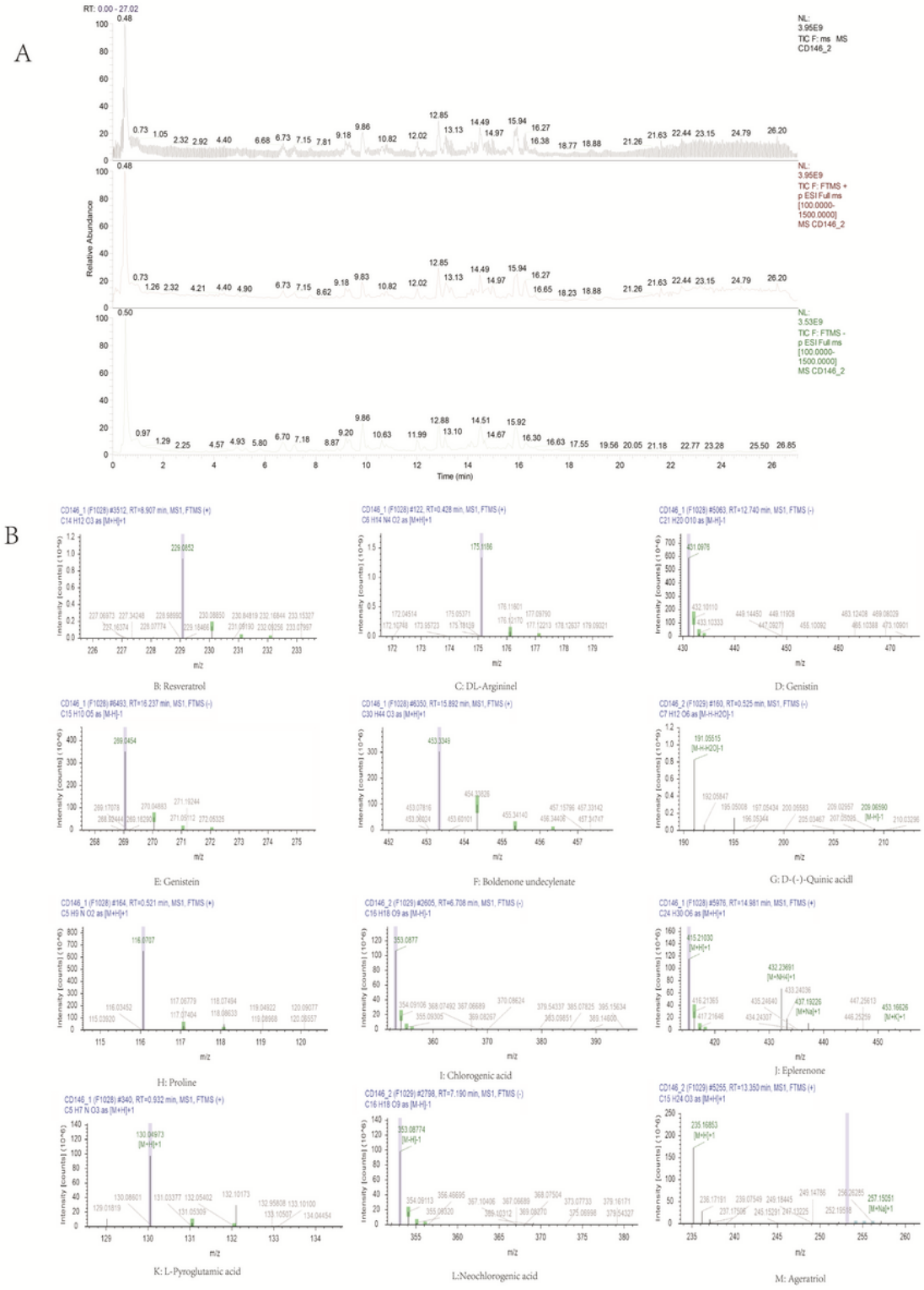

Figure 1

Identification of the main compounds of JPTQ decoction by HPLC-MS

(A).The overlay of total ion chromatogram of ESI (+) and ESI (-) mode and the ESI (+) and ESI (-) mode TIC respectively; **(B).**The relative abundance of Top 12 compounds. Based on the matching degree of multiple databases greater than 80 and the peak area.

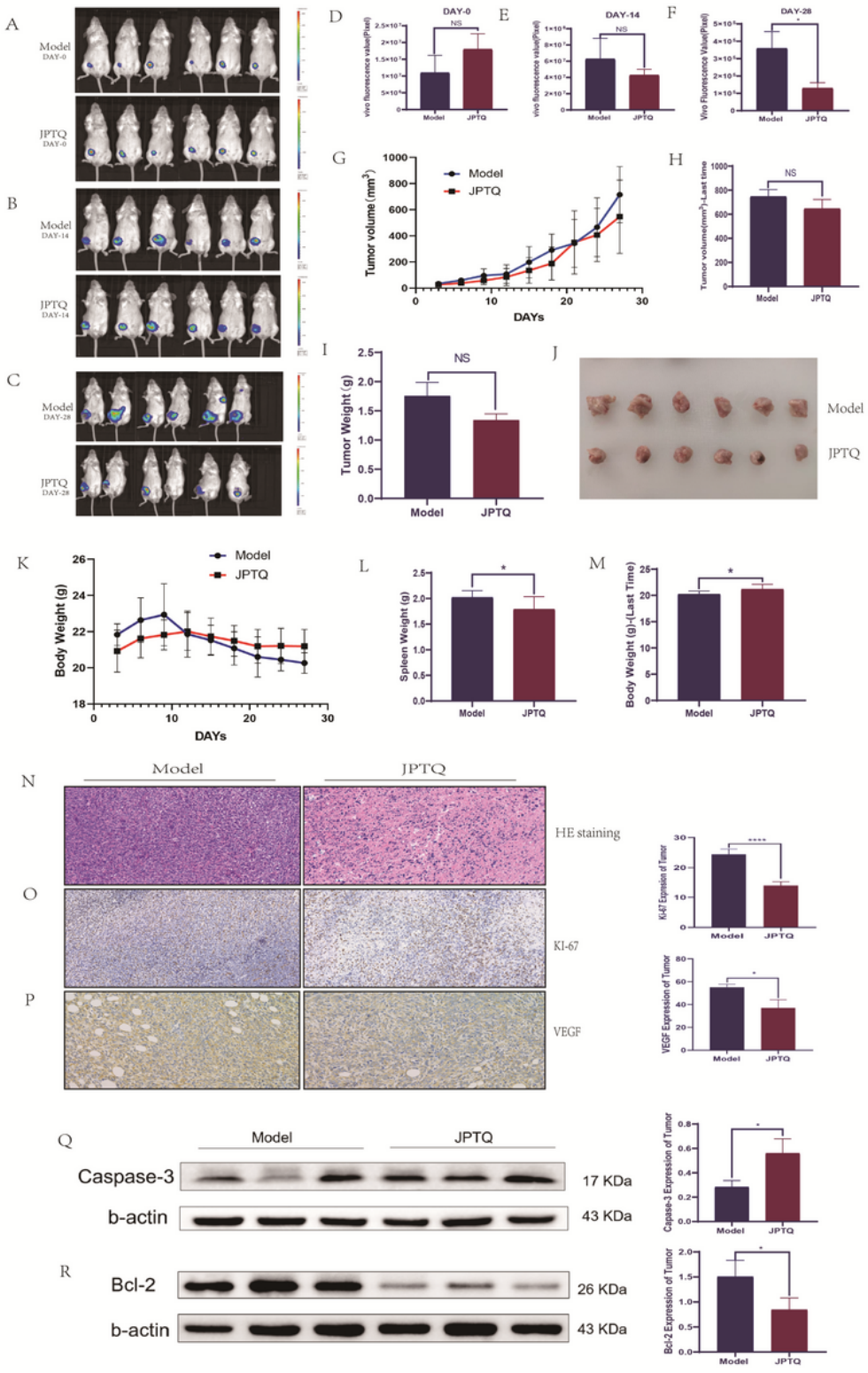

Figure 2

JPTQ decoction inhibited the proliferation of in-situ tumor and promoted its necrosis and apoptosis. **(A), (B),(C).** Biofluorescence imageing of the two groups on Day-0, Day-14,Day-28 (n=6); **(D),(E),(F)**. The vivo fluorescence Values of the two groups were compared on Day 0, Day 14 and Day 28 (n=6); **(G).**Tumor growth curve during the intervention period of JPTQ Decoction (n=8); **(H),(I)**. Comparison of tumor volume and weight between two groups (n=8) ;**(J)**.Tumor sample from two experiment groups; **(K)**. Body

weight change curve during JPTQ intervention (n=8); **(L).(M).** Comparison of spleen weight and body weight between two groups (n=8); **(N)**. Histological analysis of tumor sections stained with HE (200X) ; **(O),(P)**. Immunohistochemistry of Ki67,VEGF in Tumor tissue (200X) and the comparison of two experiment groups; **(Q),(R)**. Representative bands of Caspase-3 and Bcl-2 protein expression of tumor samples by WB analysis and the relative protein level comparison of two experiment groups; Data are expressed as a histogram of mean±SEM of three independent experiments, NS means not significant, **p*<0.05, *****p*<0.0001 vs the Model group; SEM:standard error of mean.

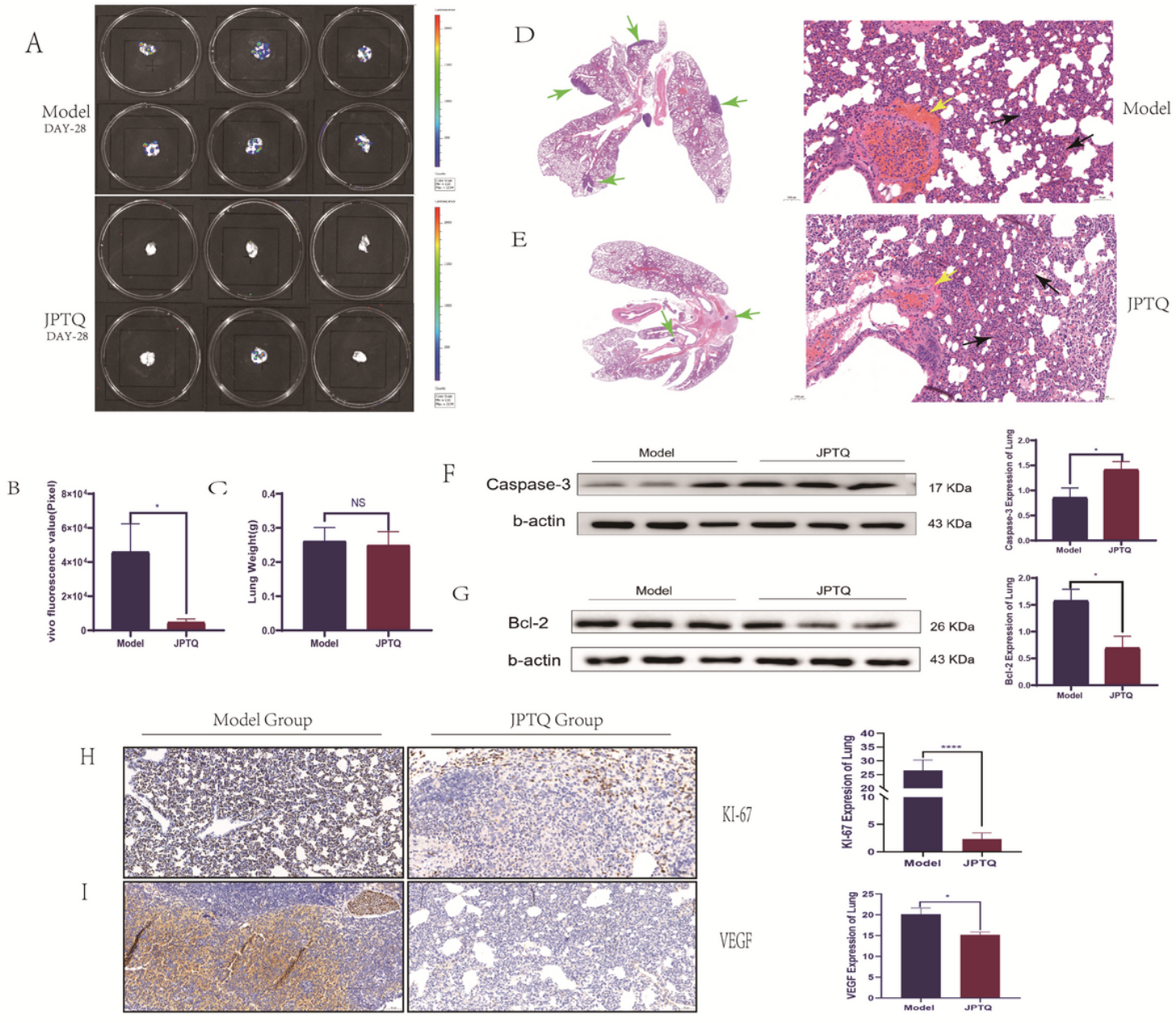

Figure 3

JPTQ decoction reduces lung metastasis of tumor bearing mice by inhibiting proliferation and promoting apoptosis. **(A)** .Biofluorescenceimageing of isolated lung tissue (n=6). **(B),(C)**. Comparison of vivo

fluorescence value and lung weight between two groups (n=6). **(D),(E)**. Lung tissue histological analysis of two experiment groups that stained with HE (200X). **(F),(G)**. Representative bands of Caspase-3 and Bcl-2 protein expression of lung tissues by WB analysis and the relative protein level comparison of two experiment groups. **(H),(I)**. Immunohistochemistry of Ki67,VEGF in lung tissue (200X) and the comparison of two experiment groups. Data are expressed as a histogram of mean±SEM of three independent experiments,NS means not significant, *p<0.05, ****p<0.0001 vs the Model group.

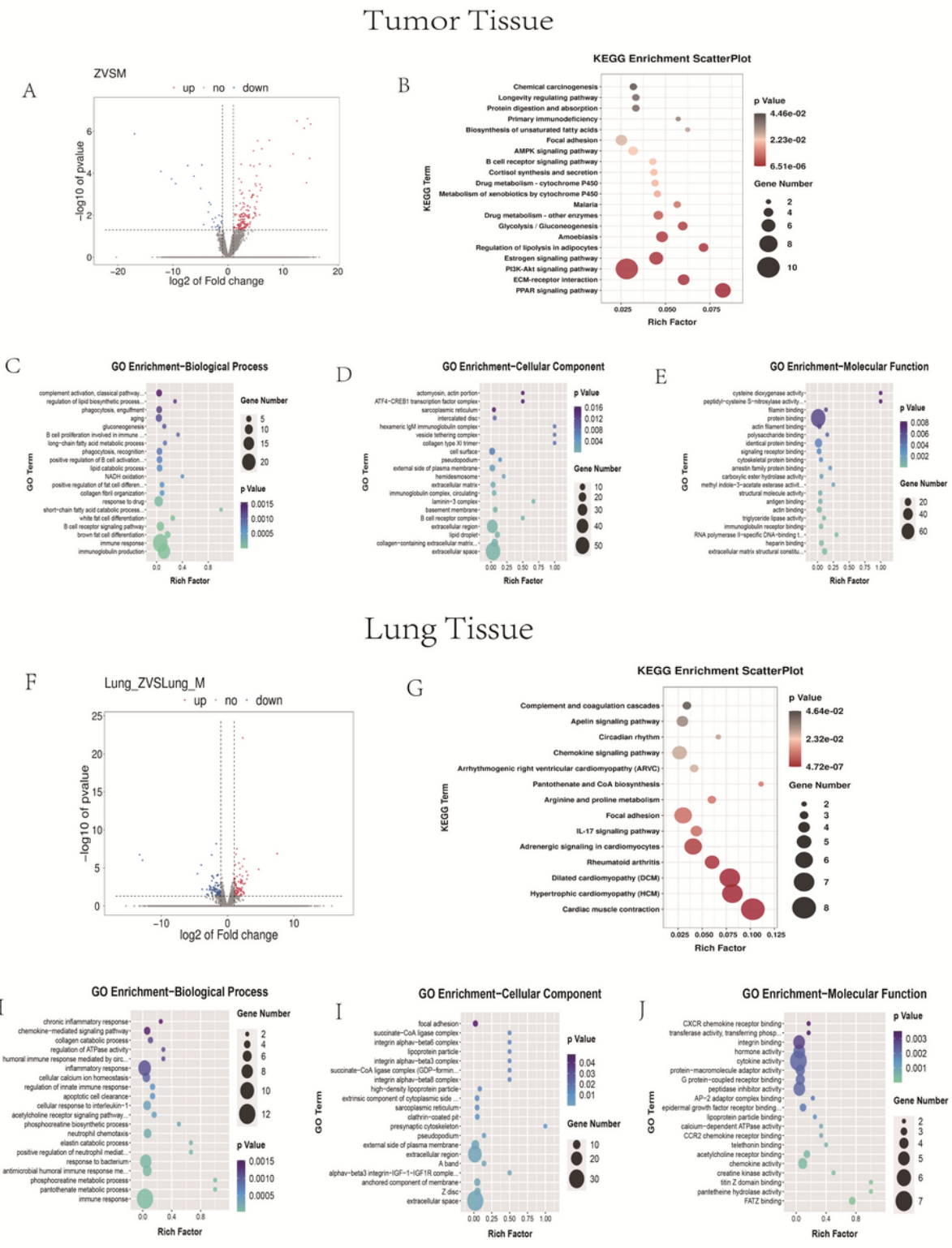

Figure 4

Transcriptome analysis of tumor tissue and tumor tissue in lung bearing mice. **(A)**.Volcano map of DEGs in tumor tissue of model group and JPTQ group (log2(Fold Change)>1, *p* value<0.05, n=4). **(B)**.KEGG Enrichment scatter plot of DEG in tumor tissue of two experiment groups (*p*<0.05 respectively). **(C),(D),(E)**. The DEG's GO Enrichment of biological processes, cellular component,molecular function in tumor tissue of two experiment groups (*p*<0.05 respectively). **(F)**.Volcano map of DEGs in lung tissue of model group and JPTQ group (log2(FoldChange)>1, *p* value<0.05, n=4). **(G)**. KEGG Enrichment scatter plot of DEG in lung tissue of two experiment groups (*p*<0.05 respectively). **(H),(I),(J)**. The DEG's GO Enrichment of biological processes, cellular component,molecular function in lung tissue of two experiment groups (*p*<0.05 respectively). DEGs:differentially expressed genes; KEGG:Kyoto Encyclopedia of Genes and Genomes; GO:Gene Ontology.

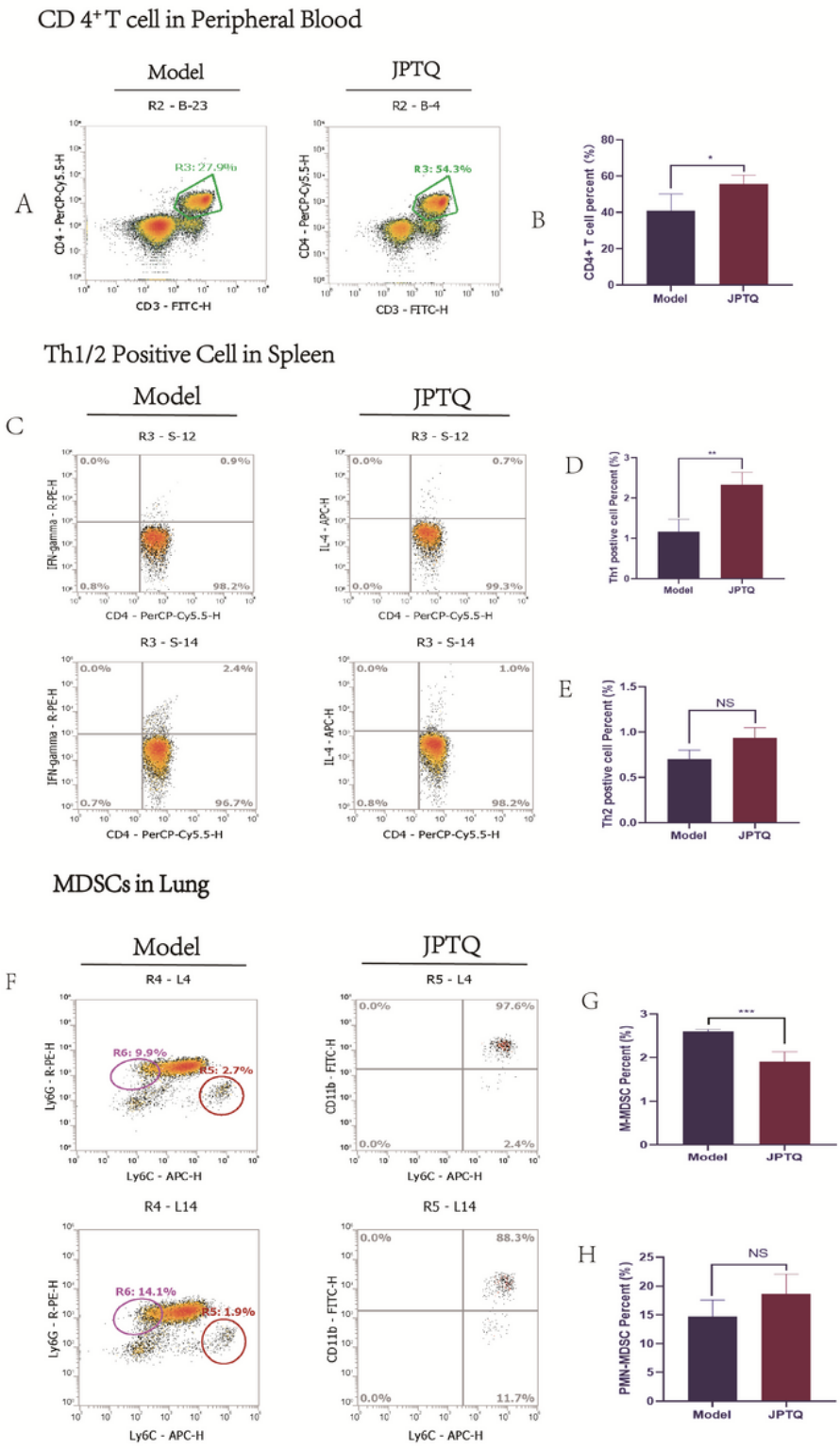

Figure 5

JPTQ decoction improved thetumor immune microenvironment of tumor bearing mice. **(A)**. CD 4^+ T cell in Peripheral Blood of tumor bearing mice in different groups (n=4); **(B)**. Comparison of CD 4^+ T cell between two experiment groups; **(C)**. Th1/2 Positive Cell in Spleen of tumor bearing mice in different groups (n=4); **(D),(E)**. Comparison of Th1 cell, Th2 cell between two experiment groups; **(F)**. MDSCs in Lung of tumor bearing mice in different groups (n=4); **(G),(H)**. Comparison of M-MDSCs,PMN-MDSCs

between two experiment groups; Data are expressed as a histogram of mean±SEM, NS means not significant, *p<0.05, **p<0.01, and ***p<0.001,****p<0.0001 vs the Model group.

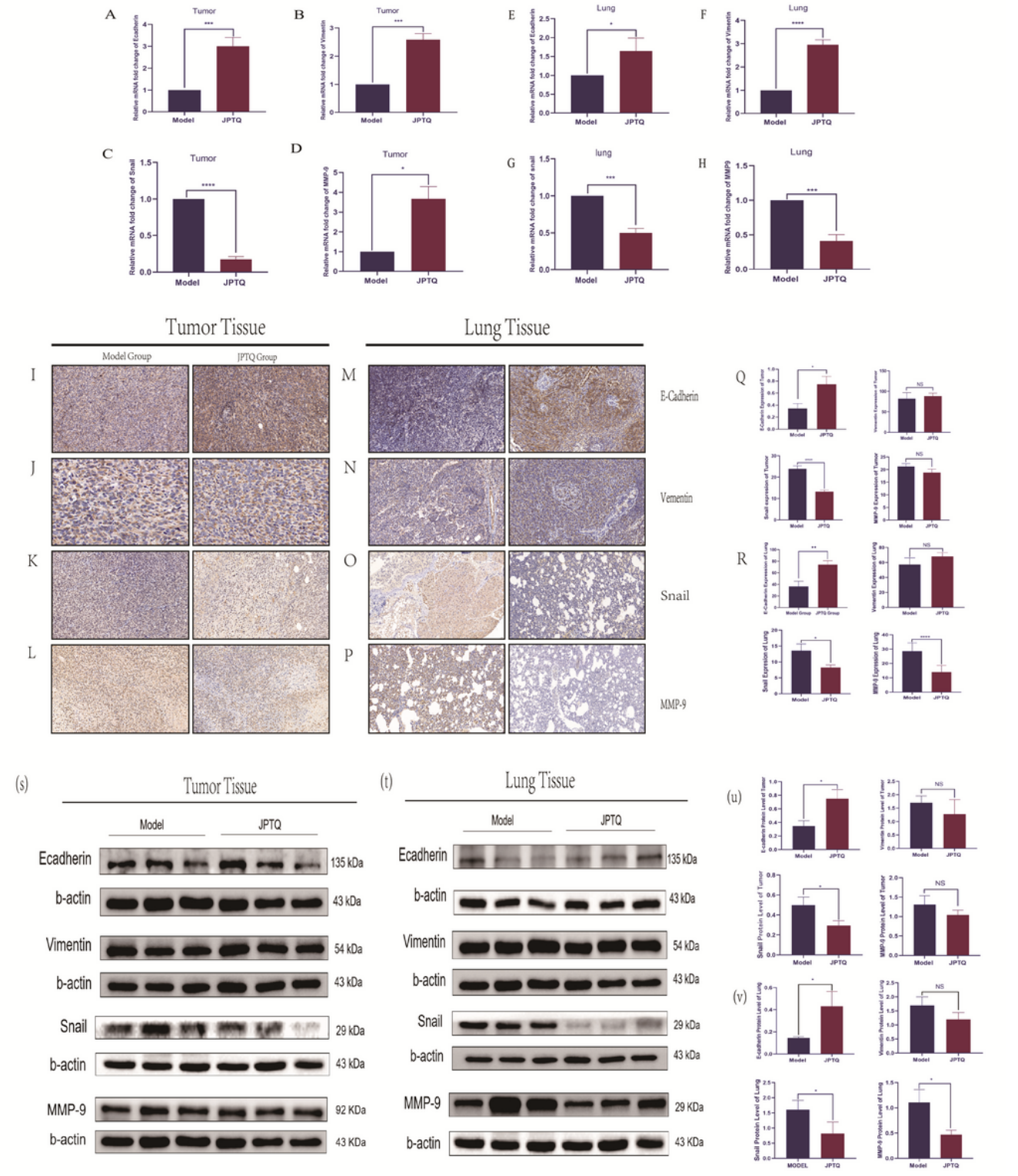

Figure 6

JPTQ decoction reduced the tumor proliferation and occurrence of lung metastasis in tumor-bearing mice by regulating the EMT process. **(A),(B),(C),(D)**. Comparison of relative mRNA fold chang of E-

Cadherin,Vimentin, Snail and MMP-9 of tumor samples; **(E),(F),(G),(H)**. Comparison of relative mRNA fold chang of E-Cadherin,Vimentin, Snail and MMP-9 of lung tissues; **(I),(J),(K),(L)**. Immunohistochemistry of E-cadherin,Vimentin, Snail, MMP-9 of tumor tissue (200X); **(M),(N),(O),(P)**. Immunohistochemistry of E-cadherin,Vimentin, Snail, MMP-9 of lung tissue (200X); **(Q)** .Comparison of E-cadherin,Vimentin, Snail, MMP-9 of tumor samples; **(R)**. Comparison of E-Cadherin,Vimentin, Snail,MMP-9 of lung tissues; **(S)**.Representative bands of E-Cadherin,Vimentin, Snail and MMP-9 protein expression of tumor samples by WB analysis; **(T)**. Representative bands of E-Cadherin,Vimentin, Snail and MMP-9 protein expression of lung tissues by WB analysis; **(U)**.The relative protein level comparison of E-Cadherin,Vimentin,Snail and MMP-9 of tumor samples; **(V)**. The relative protein level comparison of E-Cadherin,Vimentin, Snail and MMP-9 of lung tissues; Data are expressed as a histogram of mean±SEM of three independent experiments, NS means not significant, *p<0.05, **p <0.01, and****p<0.0001 vs the Model group. EMT: epithelial-mesenchymal transition; MMP-9: matrix metalloprotein 9; WB:western blot; SEM:standard error of mean.

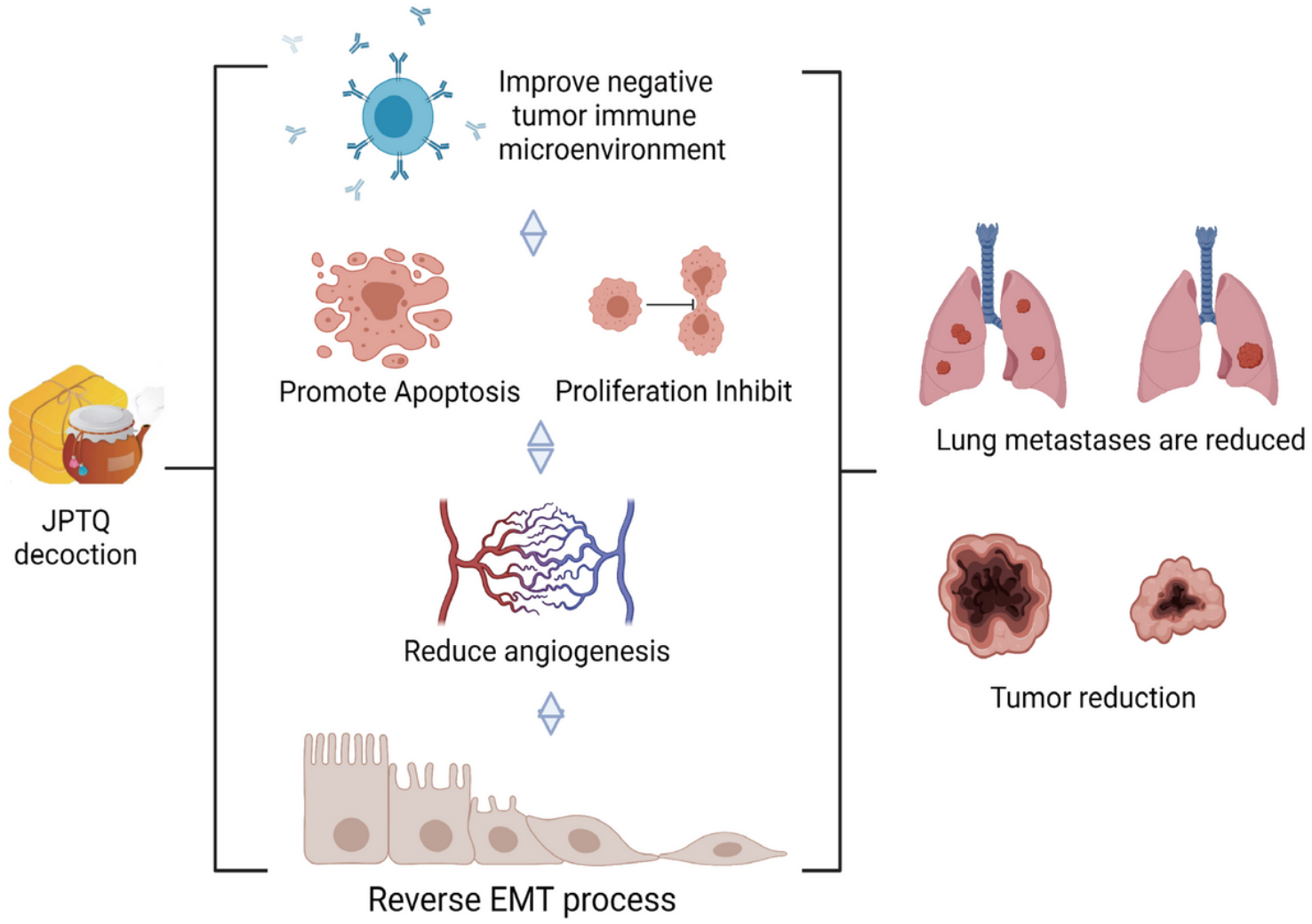

Figure 7

Comprehensive analysis of the anti tumor-proliferation and anti lung-metastasis mechanism of JPTQ decoction

Supplementary Files

This is a list of supplementary files associated with this preprint. Click to download.

- SupplementarytablesS1S2.xls